Robust future changes in meteorological drought in CMIP6 projections despite uncertainty in precipitation

Anna M Ukkola[1], Martin G De Kauwe[2], Michael L. Roderick[1], Gab Abramowitz[2], and Andy J Pitman[2]

[1]Australian National University
[2]University of New South Wales

November 24, 2022

Abstract

Quantifying how climate change drives drought is a priority to inform policy and adaptation planning. We show that the latest Coupled Model Intercomparison Project (CMIP6) simulations project coherent regional patterns in meteorological drought for two emissions scenarios to 2100. We find robust projected changes in seasonal drought duration and frequency (robust over >45% of the global land area), despite a lack of agreement across models in projected changes in mean precipitation (24% of the land area). Future drought changes are larger and more consistent in CMIP6 compared to CMIP5. We find regionalised increases and decreases in drought duration and frequency that are driven by changes in both precipitation mean and variability. Conversely, drought intensity increases over most regions but is not simulated well historically by the climate models. The more robust projections of meteorological drought compared to mean precipitation in CMIP6 provides significant new opportunities for water resource planning.

Robust future changes in meteorological drought in CMIP6 projections despite uncertainty in precipitation

Anna M. Ukkola[1], Martin G. De Kauwe[2,3], Michael L. Roderick[1], Gab Abramowitz[2] and Andrew J. Pitman[2]

[1]ARC Centre of Excellence for Climate Extremes and Research School of Earth Sciences, Australian National University, Canberra, ACT, Australia
[2]ARC Centre of Excellence for Climate Extremes and Climate Change Research Centre, University of New South Wales, Sydney, NSW, Australia
[3]Evolution and Ecology Research Centre, University of New South Wales, Sydney, NSW 2052, Australia

Corresponding author: A.M. Ukkola (a.ukkola@unsw.edu.au)

For submission to *Geophysical Research Letters*

Key points:

- Quantifying meteorological droughts using changes in both the mean and variability of precipitation leads to more robust projections
- CMIP6 projections show robust changes in the frequency and duration of seasonal meteorological drought over > 45% of the global land area
- Future drought changes are larger and more consistent in CMIP6 compared to CMIP5

Abstract

Quantifying how climate change drives drought is a priority to inform policy and adaptation planning. We show that the latest Coupled Model Intercomparison Project (CMIP6) simulations project coherent regional patterns in meteorological drought for two emissions scenarios to 2100. We find robust projected changes in seasonal drought duration and frequency (robust over >45% of the global land area), despite a lack of agreement across models in projected changes in mean precipitation (24% of the land area). Future drought changes are larger and more consistent in CMIP6 compared to CMIP5. We find regionalised increases and decreases in drought duration and frequency that are driven by changes in both precipitation mean and variability. Conversely, drought intensity increases over most regions but is not simulated well historically by the climate models. The more robust projections of meteorological drought compared to mean precipitation in CMIP6 provides significant new opportunities for water resource planning.

Plain language summary

Understanding how climate change affects droughts guides adaptation planning in agriculture, water security and ecosystem management. Earlier climate projections have highlighted high uncertainty in future drought projections, hindering effective planning. We use the latest projections and find more robust projections of meteorological drought compared to mean precipitation. These more robust projections provide clearer direction for water resource planning and the identification of agricultural and natural ecosystems at risk.

1 Introduction

Droughts cause significant economic, social and ecosystem impacts worldwide (IPCC, 2014). Many devastating droughts have occurred in recent decades, such as those in California (Griffin & Anchukaitis, 2014), the Horn of Africa (Chris Funk et al., 2019), Europe (Ciais et al., 2005) and Australia (van Dijk et al., 2013), risking regional food and water security. Between 1998 and 2017, droughts are estimated to have impacted 1.5 billion people and accounted for a third of all natural disaster impacts (United Nations, n.d.; *Funk et al.*, 2019a). Climate change may be increasing the severity and frequency of droughts (Dai, 2013; Trenberth et al., 2014), posing challenges for water management, agriculture and natural ecosystems. Understanding how droughts will change under increasing greenhouse gas concentrations is therefore an urgent research question of widespread importance.

A lack of precipitation is the primary cause of drought (McKee et al., 1993). Climate change can influence precipitation (meteorological) droughts through changes in atmospheric water holding capacity, circulation patterns and moisture supply. Globally, coupled climate models project an increase in precipitation of ~2% for every 1°C of warming (Held & Soden, 2006), with stronger and sometimes opposing changes regionally, but also simulate changes in the frequency and intensity of precipitation events (Sillmann et al., 2013). More intense but less frequent precipitation events have been observed across many regions (Donat et al., 2019), with projections of an increased incidence of extreme precipitation events coupled with longer dry spells (Sillmann et al., 2013). Changes in atmospheric dynamics and modes of variability such as El Niño Southern Oscillation can further influence regional precipitation patterns (Trenberth et al., 2014), together with changes in evapotranspiration which shows contrasting trends over land and oceans (Roderick et al., 2014). Meteorological droughts are negative anomalies in water supply and changes in droughts at regional scales thus result from complex interactions of the different processes influencing long-term precipitation totals and variability (Sheffield & Wood, 2011).

It is widely reported that droughts and aridity will worsen under increasing greenhouse gas concentrations (Dai, 2013; Dai et al., 2018; Mirzabaev et al., 2019; Park et al., 2018; Sherwood & Fu, 2014) but this is not supported by recent observations of precipitation (Funk et al., 2019; Orlowsky & Seneviratne, 2013) and other hydrological quantities, including runoff, actual evapotranspiration and pan evaporation (Roderick & Farquhar, 2002; Scheff, 2018; Ukkola & Prentice, 2013). The previous suggestions of more severe droughts largely arises from uncoupled modelling studies (Sheffield et al., 2012) that do not capture the various climate interactions and generally quantify droughts using potential evapotranspiration in addition to precipitation (Dai, 2013). Recent studies (Greve et al., 2019; Milly & Dunne, 2016; Justin Sheffield et al., 2012; Swann et al., 2016; Yang et al., 2019) have shown that these uncoupled approaches strongly overestimate regional drought and aridity increases due to inappropriate assumptions under increasing CO_2 and are inconsistent with coupled climate model projections. As such, those studies have encouraged the use of direct climate model outputs in drought assessments. Previous studies analysing droughts from climate models have often quantified drought from mean precipitation and/or other water balance components (Lehner et al., 2017; Swann et al., 2016), or by analysing the full range (i.e. negative and positive anomalies) of indices such as Standardised Precipitation Index (Orlowsky & Seneviratne, 2013), and have concluded uncertain, "elusive" trends in droughts (Collins et al., 2013; Hoegh-Guldberg et al., 2018; Orlowsky & Seneviratne, 2013). However, it has been suggested that quantifying droughts from percentiles instead of mean values would allow a better characterisation of the changes in drought (Trenberth et al., 2014).

We quantify projected changes in meteorological droughts using the new state-of-the-art CMIP6 climate model projections (Eyring et al., 2016) that underpin the 6th Intergovernmental Panel on Climate Change assessment report. We use nine models from CMIP6 and contrast those with equivalent models from the previous generation of projections from CMIP5 (Taylor et al., 2012). We characterise meteorological droughts as seasonal-scale negative precipitation anomalies. Drought impacts depend on their duration, intensity and frequency (Sheffield & Wood, 2011) and we quantify future changes in these key characteristics.

2 Materials and Methods

2.1 Data

For observed precipitation, we used three global products at 0.5° resolution that cover the period 1950-2014. These were monthly time series products by the Climatic Research Unit (CRU TS4.02) (Harris et al., 2014) and Global Precipitation Climatology Centre (GPCC; version 2018) (Schneider et al., 2016) as well as the daily product Rainfall Estimate of a Gridded Network (REGEN) (Contractor et al., 2020).

For modelled precipitation, we obtained monthly simulations of total precipitation (variable *pr*) from the Coupled Model Intercomparison Project phases 5 and 6 (CMIP5 and CMIP6, respectively). We used the historical experiment, as well as two future scenarios reaching radiative forcing of 4.5 and 8.5 W m^{-2} by 2100 from each project. These radiative forcing levels were chosen as they are available for both CMIP5 and CMIP6. For CMIP6, the two future scenarios used were the Shared Socioeconomic Pathways (SSP) 2-4.5 and 5-8.5. SSP2-4.5 represents an intermediate "middle of the road" scenario and SSP5-8.5 is a high emissions "fossil-fuelled development" scenario (O'Neill et al., 2016). For CMIP5, the two scenarios used were the Representative Concentration Pathways (RCP) 4.5 and 8.5 (van Vuuren et al., 2011). Results for the higher 8.5 W m^{-2} scenario are presented in the main paper and for the 4.5 W m^{-2} scenario in Supplementary Figures S7-9.

We used nine models from each project that were common to both CMIP6 and CMIP5 to enable comparison between projections from the two projects (Table S1). We also present the full CMIP5 range in Figure S1 using all available models that report precipitation for the historical and future scenarios (31 models and 71 individual model realisations; Table S2). These results are consistent with the subset of nine models, suggesting our results are representative of the full CMIP5 uncertainty and not an artefact of model selection. For each model, all ensemble members that were available for both historical and future experiments were used to better account for internal variability. Ensemble members used for each model are listed in Tables S1 and S2. We calculated all drought metrics at the models' native resolution and regridded the outputs to a common 1° resolution for plotting using bilinear interpolation. As a land-sea mask was not available for all models, the global land area was determined as the common pixels across the three observational datasets and used to mask model outputs. Land pixels for which drought metrics could not be determined from observations (mainly due to non-varying precipitation in the CRU dataset) were masked out from all analyses.

2.2 Defining droughts

Many definitions of drought exist. Here we only consider meteorological droughts (rainfall deficits) as these can be underpinned by long-term global observations. Lack of rainfall is usually the primary cause of other types of drought, such as hydrological (streamflow) and agricultural (soil moisture or yield) droughts (McKee et al., 1993). Global climate models also show better agreement and higher skill for precipitation droughts compared with runoff and soil moisture droughts (Ukkola et al., 2018). Despite being a common method for defining droughts, we do not use a metric that includes potential evapotranspiration (PET), such as Standardised Precipitation Evapotranspiration Index (Vicente-Serrano et al., 2010), as the use of PET has been shown to lead to overestimation of future drought compared to direct climate model outputs (Milly & Dunne, 2016; Sheffield et al., 2012; Swann et al., 2016; Yang et al., 2019) and double-counting of the effects of surface humidity and temperature on droughts (Swann et al., 2016). Rather, the effect of climate change, including temperature and vapour pressure deficit increase, is included in our study through the feedbacks within climate models on the water cycle and consequently on precipitation.

We use percentile thresholds to determine drought periods as this method involves no assumptions about the data distribution. We use the 15th percentile as the drought threshold, such that any month below this threshold is classified as drought. The 15th percentile corresponds approximately to a threshold of −1 for the widely used Standardised Precipitation Index (McKee et al., 1993) (SPI) and is commonly used to characterise "moderate" droughts (McKee et al., 1993). We use this threshold to ensure we have a sufficient number of drought events to infer trends in drought metrics reliably. Previous work has shown that whilst simulated drought characteristics can be somewhat sensitive to the choice of threshold, inter-model differences represent a much greater source of uncertainty (Ukkola et al., 2018).

We first converted the monthly precipitation time series into 3-month running means to smooth out short-term variations. This is analogous to calculating SPI at scale 3 and reflects changes in seasonal droughts, which have widespread impacts on ecosystems, agriculture and water resources in many tropical and temperate regions (Ciais et al., 2005; Lewis et al., 2011; Saleska et al., 2007). Using the 3-monthly running means also incorporates soil moisture "memory" effects (Orth & Seneviratne, 2012). However, for completeness we also present results for 12-month running means in the Supplementary Information for annual-scale droughts (Figure S10-12), which are more relevant in water-limited environments adapted to short-term droughts and found these results to be largely qualitatively consistent with the changes in seasonal droughts.

We then define the 15th percentile threshold separately for each month to account for seasonality. We use the period 1950-2014 to determine the monthly percentile thresholds so that all drought metrics are relative to this historical baseline period. We use this 65-year period to define the thresholds instead of commonly used 30-year periods to better account for climate variability, which should allow for more reliable determination of the percentiles and therefore drought. We chose 1950 as the start year as the three observational rainfall products used here become available then and are generally more reliable ~1950s onwards (Sun et al., 2012) (for CESM1-WACCM, 1955 was used as the start year as this is the first available year in the historical simulation). As CMIP6 historical simulations finish in 2014, this was chosen as the end year for the baseline period. CMIP5 historical simulations finish in 2005 and were extended with the RCP8.5 scenario to calculate the thresholds.

2.3 Drought metrics

We calculated three common droughts metrics: duration, intensity and frequency (Sheffield & Wood, 2011). Duration (D; months) was defined as the number of consecutive months below the drought threshold and frequency is the number of drought events over a time period. Intensity (I; mm month^{-1}) is the difference between the drought threshold ($x_{15,m}$; mm) and the monthly precipitation value (x_m; mm), averaged over all months during a drought event:

$$I = \frac{\sum(x_{15,m} - x_m)}{D}; m \in [i, j] \quad (1)$$

where i is the drought start month and j the end month.

2.4 Statistical methods

We defined projections as "robust" when the magnitude of the multi-model mean future change exceeded the inter-model standard deviation of the change (Meehl et al., 2007). All multi-model means and standard deviations were weighted to account for the different number of ensemble members for individual models by assigning each model realisation a weight of $1/n$, where n is the total number of ensemble members for that model.

For the regional case studies in Figure 3, we used a paired t-test weighted for ensemble members to assess the significance of multi-model mean changes in the mean and standard deviation of monthly precipitation from the historical baseline period to the 2050-2100 future period. The t-test was performed using the R package "*weights*" (https://cran.r-project.org/web/packages/weights/weights.pdf).

3 Results

3.1 Projected changes in drought characteristics

Focusing first on the historical period, models compare well with observed drought duration over most regions, with the exception of the tropics (see stippling in Figure 1a). This suggests good model skill in simulating drought duration (Ukkola et al., 2018), increasing confidence in the projections. Many subtropical regions are projected to experience longer drought durations in 2051-2100 compared to the historical baseline period (Figure 1c). The strongest, most robust increases are projected in Central America, Chile, the Mediterranean, southern Australia and southern and western Africa, with increases in drought duration from ~2 months during the historical period to ~4 months in the future. Strong increases are also projected over the Amazon but models show lower skill in capturing observed drought durations in this region (Figure 1a,b). By contrast, shorter droughts are projected in central Sahel, eastern Russia, northern China and northern high latitudes, with declines up to 1 month. Overall, the pattern of drought duration changes is similar between CMIP6 and CMIP5, but the changes in CMIP6 are stronger and more robust compared to the nine equivalent CMIP5 models as well as the full CMIP5 range (increased model agreement, Figure 1c,d and S1). In particular, model agreement in CMIP6 is higher over Australia, the Mediterranean, Central America, Chile and Amazon, but lower over parts of central Russia. Projected changes in drought frequency show a similar footprint to duration, with the models generally capturing the observed frequency well over the historical period, except over the tropics (Figure S2a). Fewer drought events are projected in the northern mid- to high latitudes and eastern Sahel and more frequent droughts in the subtropics and the Amazon (Figure S2b).

Projected changes in drought intensity suggest an increasing trend over several regions, with some differences in spatial patterns compared to duration. The largest intensification of droughts is predicted in the tropics, including the Amazon, central Africa and southeast Asia, as well as Chile and Central America (Figure 2c). These increases are much stronger and more robust in CMIP6 compared to CMIP5 (Figure 2c,d). Droughts are also projected to intensify over Europe and the Mediterranean. In the U.S. and western Russia, projections of drought duration remain uncertain but models show robust increases in intensity. Conversely, over southern Africa, Australia and northwest North America, models agree on projected changes in duration but not intensity. In northern mid- and high latitudes, droughts are projected to become shorter but more intense. However, neither CMIP6 nor CMIP5 simulations show good agreement with observations (see lack of stippling in Figure 2a,b), suggesting low model skill over most of the world in simulating drought intensity. The evaluation of model skill is, however, complicated by higher observational uncertainty for intensity compared to other drought metrics, especially in the tropics and sub-tropics (Figure S3). Capturing intensity correctly requires skilful simulation of both mean precipitation and variability and previous work (Ukkola et al., 2018) has shown systematic biases in CMIP5 in both metrics, in particular an underestimation of monthly precipitation variability relative to its mean (i.e. coefficient of variation) in humid regions. Figure S4 suggests that model biases in drought intensity remain similar in CMIP6 compared to CMIP5, suggesting future projections of drought intensity should be interpreted with caution, particularly over the tropics.

The above results consider uncertainties in drought projections arising from model responses (structure & parameterisation). The emissions scenarios represent another source of uncertainty in the drought projections. Overall, the spatial patterns for future drought changes in the lower 4.5 W m^{-2} emissions scenarios are consistent with the higher 8.5 W m^{-2} scenario (Figures S7-S9). However, the changes are smaller in magnitude and less robust in the 4.5 W m^{-2} scenario. The global land area showing robust changes under the lower emissions scenario decreases from 45% to 36% for duration, from 26% to 10% for intensity and 57% to 52% in frequency in the CMIP6 models compared to the higher scenario. This suggests some of the future changes in drought could be mitigated through lower greenhouse emissions. However, robust changes especially in drought duration and frequency are projected over many regions even under the lower emissions scenario.

Internal variability, i.e. the natural variability independent of external forcing, presents a third major source of uncertainty in climate change projections (Deser et al., 2010) and must be accounted for when assessing changes in drought (Trenberth et al., 2014). We analysed all available model ensemble members that were common to the historical and future experiments over five hotspot regions to explore the robustness of the projections to internal variability (Figure S5; see Figure 3 for regions). Individual ensemble members differ in the magnitude of change, but the direction of change is highly consistent within ensemble members for individual models over all regions. This suggests that the projected changes are a robust feature of each model's projections and agrees with previous work which showed that internal variability is a minor source of uncertainty in drought metrics compared to inter-model differences during the historical period (Ukkola et al., 2018).

3.2 Role of mean and variability changes

Changes in future drought can arise from both changes in precipitation mean and variability (Trenberth et al., 2014). We explored mean and variability changes as the drivers of future drought by analysing changes in the mean and standard deviation of monthly precipitation (Figure 3). Mean precipitation shows both increases and decreases, whereas precipitation variability is largely increasing, in line with previous studies (Figure 3; Collins et al., 2013; Pendergrass et al., 2017). Broadly, changes in drought duration correspond to changes in mean precipitation, but intensity changes are driven by both the mean and variability (cf. Figure 1c, 2c and 3a,b). The Mediterranean and southern Africa represents regions where increased drought duration and intensity are primarily driven by declines in mean monthly precipitation, even though mean precipitation changes are less robust than those in the drought metrics (Figure 3c). In the Mediterranean, mean precipitation is projected to decline by 14% ($p = 0.002$ from a paired t-test; see Methods) under the higher emissions scenario and in southern Africa by 9% ($p = 0.050$). Other similar regions include Chile and Central America. By contrast, over central Europe, the models simulate a small increase in mean precipitation of 3% ($p = 0.040$) but a concurrent 18% increase in drought intensity ($p < 0.0001$). This can be attributed to an increase in standard deviation by 37% ($p < 0.0001$) (Figure 3d,g). Similarly, over Australia, model agreement on mean precipitation change is low (Figure 3a) but standard deviation is projected to increase by 13% ($p = 0.028$), with concurrent increases in drought intensity and duration when averaged over the region (21%, $p < 0.0001$ and 20%, $p < 0.001$, respectively).

The Amazon presents an interesting example where drought projections are partly driven by both mean and variability changes. Mean precipitation is projected to decline by 7% and standard deviation increase by 11% but neither change is statistically significant ($p = 0.179$ and $p = 0.122$, respectively) (Figure 3e,h). Yet, drought duration and intensity changes are highly significant ($p < 0.0001$), highlighting the need to consider both mean and variability when assessing drought changes. Overall, changes in seasonal drought duration, intensity and frequency are robust over 45%, 26% and 57% of the global land area (excluding Antarctica) in CMIP6, respectively (i.e. the magnitude of the multi-model mean future change exceeds the inter-model standard deviation; Methods). The level of model agreement is higher compared to CMIP5 which shows robust changes over 31%, 10% and 51% of the land area, respectively. By contrast, changes in mean precipitation in CMIP6 are robust over 24% of the land area, indicating more robust projections of drought than mean precipitation. These results suggest that using long-term mean precipitation to quantify drought changes is insufficient and leads to lower confidence in future drought projections.

4 Discussion and Conclusions

CMIP6 models indicate robust future changes in droughts in hot spot regions such as the Amazon, the Mediterranean and northern mid- and high latitude regions, despite uncertainty in the magnitude of changes. The models project widespread increases in drought intensity but at regional scales the projections for meteorological drought duration and frequency are more nuanced. Longer or more intense droughts are projected in the high biomass regions of the Amazon and northern boreal zone, with potential implications for ecosystem function and long-lived carbon sinks. However, some of the negative drought impacts may be buffered by vegetation adaptions and/or increased vegetation water use efficiency under elevated CO_2 (Swann et al., 2016). Similarly, more intense droughts are projected over several agricultural regions, including Chile, central Europe, eastern U.S. and parts of China, exposing these key food basket regions to potential economic losses. Some highly populated, water scarce regions, such as the Mediterranean, southern and western Africa and southern North America are projected to experience more severe droughts, risking water and food security. In other dry regions, in particular eastern Sahel which has experienced devastating droughts in the past (Sheffield & Wood, 2011), climate models project less severe droughts in the future.

Projections of mean precipitation have remained highly uncertain over many land areas (Collins et al., 2013). Surprisingly, our study shows more robust projections of meteorological droughts than mean precipitation. This result indicates that the common approach of using mean precipitation to quantify drought changes leads to lower confidence in future drought projections. The more robust drought projections over many hotspot regions provide significant opportunities for policy interventions and adaptation decisions to improve water security under climate change. Our results highlight how changes in drought are increasingly consistent, and hot spot regions are increasingly clear in newer CMIP projects and several attributes of drought are now consistently simulated by climate models. This offers considerable potential for evidence-based strategies to enhance water and food security and the identification of regions with high value ecosystems at risk from increased drought. Finally, we note that the projected changes in droughts are stronger under the higher emissions scenario; future drought risk in hot spot regions would be mitigated by reducing greenhouse gas emissions.

Acknowledgements

The research was funded by the Australian Research Council Centre of Excellence for Climate Extremes (CE170100023). MDK acknowledges support from the NSW Research Attraction and Acceleration Program and MDK and AJP also acknowledge the ARC Discovery Grant (DP190101823). We are grateful to the National Computational Infrastructure at the Australian National University and the Earth System Grid Federation for making the CMIP6 and CMIP5 model outputs available. We acknowledge the World Climate Research Programme, which, through its Working Group on Coupled Modelling, coordinated and promoted CMIP6 and CMIP5. We thank the climate modelling groups for producing and making available their model output, the Earth System Grid Federation (ESGF) for archiving the data and providing access, and the multiple funding agencies who support CMIP6, CMIP5 and ESGF. The CMIP6 and CMIP5 outputs used in this study are available from the Earth System Grid Federation (https://esgf-node.llnl.gov). The observed precipitation datasets can be obtained from CRU (http://www.cru.uea.ac.uk/data/), GPCC (https://www.dwd.de/EN/ourservices/gpcc/gpcc.html) and REGEN (https://researchdata.ands.org.au/rainfall-estimates-gridded-v1-2019/1408744/). The analysis

codes are available at https://github.com/aukkola/CMIP5_on_NCI and https://bitbucket.org/aukkola/cmip6_drought_projections.

References

Ciais, P., Reichstein, M., Viovy, N., Granier, A., Ogée, J., Allard, V., et al. (2005). Europe-wide reduction in primary productivity caused by the heat and drought in 2003. *Nature*, *437*, 529–533.

Collins, M., Knutti, R., Arblaster, J., Dufresne, J. L., Fichefet, T., Friedlingstein, P., et al. (2013). Long-term Climate Change: Projections, Commitments and Irreversibility. In T. F. Stocker, D. Qin, G.-K. Plattner, M. Tignor, S. K. Allen, J. Boschung, et al. (Eds.), *Climate Change 2013: The Physical Science Basis. Contribution of Working Group I to the Fifth Assessment Report of the Intergovernmental Panel on Climate Change* (pp. 1029–1136). Cambridge, United Kingdom and New York, NY, USA: Cambridge University Press.

Contractor, S., Donat, M. G., Alexander, L. V., Ziese, M., Meyer-Christoffer, A., Schneider, U., et al. (2020). Rainfall Estimates on a Gridded Network (REGEN) - A global land-based gridded dataset of daily precipitation from 1950-2013. *Hydrology and Earth System Sciences*, *24*, 919–943.

Dai, A. (2013). Increasing drought under global warming in observations and models. *Nature Climate Change*, *3*, 52–58.

Dai, A., Zhao, T., & Chen, J. (2018). Climate Change and Drought: a Precipitation and Evaporation Perspective. *Current Climate Change Reports*, *4*, 301–312.

Deser, C., Phillips, A., Bourdette, V., & Teng, H. (2010). Uncertainty in climate change projections: the role of internal variability. *Climate Dynamics*, *38*, 527–546.

van Dijk, A. I. J. M., Beck, H. E., Crosbie, R. S., de Jeu, R. a. M., Liu, Y. Y., Podger, G. M., et al. (2013). The Millennium Drought in southeast Australia (2001-2009): Natural and human causes and implications for water resources, ecosystems, economy, and society. *Water Resources Research*, *49*, 1–18.

United Nations Office for Disaster Risk Reduction and Centre for Research on the Epidemiology of Disasters (n.d.). *Economic losses, poverty and disasters 1998-2017*.

Donat, M. G., Angélil, O., & Ukkola, A. M. (2019). Intensification of precipitation extremes in the world’s humid and water-limited regions. *Environmental Research Letters*, *14*, 065003.

Eyring, V., Bony, S., Meehl, G. A., Senior, C. A., Stevens, B., Stouffer, R. J., & Taylor, K. E. (2016). Overview of the Coupled Model Intercomparison Project Phase 6 (CMIP6) experimental design and organization. *Geoscientific Model Development*, *9*, 1937–1958.

Funk, C, Harrison, L., Alexander, L., Peterson, P., Behrangi, A., & Husak, G. (2019). Exploring trends in wet-season precipitation and drought indices in wet, humid and dry regions. *Environmental Research Letters*.

Funk, Chris, Shukla, S., Thiaw, W. M., Rowland, J., Hoell, A., McNally, A., et al. (2019). Recognizing the Famine Early Warning Systems Network: Over 30 Years of Drought Early Warning Science Advances and Partnerships Promoting Global Food Security. *Bulletin of the American Meteorological Society*, *100*, 1011–1027.

Greve, P., Roderick, M. L., Ukkola, A. M., & Wada, Y. (2019). The Aridity Index under global warming. *Environmental Research Letters*.

Griffin, D., & Anchukaitis, K. J. (2014). How unusual is the 2012–2014 California drought ? *Geophysical Research Letters*, *41*, 9017–9023.

Harris, I., Jones, P. D., Osborn, T. J., & Lister, D. H. (2014). Updated high-resolution grids of monthly climatic observations - the CRU TS3.10 Dataset. *International Journal of Climatology*, *34*, 623–642.

Held, I. M., & Soden, B. J. (2006). Robust Responses of the Hydrological Cycle to Global Warming. *Journal of Climate*, *19*, 5686–5699.

Hoegh-Guldberg, Jacob, O. D., Taylor, M., Bindi, M., Brown, S., Camilloni, I., et al. (2018). Impacts of 1.5°C of Global Warming on Natural and Human Systems. In V. Masson-Delmotte, P. Zhai, H.-O. Pörtner, D. Roberts, J. Skea, P. R. Shukla, et al. (Eds.), *Global Warming of 1.5°C. An IPCC Special Report on the impacts of global warming of 1.5°C above pre-industrial levels and related global greenhouse gas emission pathways, in the context of strengthening the global response to the threat of climate change,* (pp. 175–311). Retrieved from https://www.ipcc.ch/sr15

IPCC. (2014). *Climate Change 2014: Impacts, Adaptation, and Vulnerability. Part A: Global and Sectoral Aspects. Contribution of Working Group II to the Fifth Assessment Report of the Intergovernmental Panel on Climate Change*. (C. B. Field, V. R. Barros, D. J. Dokken, K. J. Mach, M. D. Mastrandrea, T. E. Bilir, et al., Eds.). Cambridge, United Kingdom and New York, NY, USA: Cambridge University Press.

Lehner, F., Coats, S., Stocker, T. F., Pendergrass, A. G., Sanderson, B. M., Raible, C. C., & Smerdon, J. E. (2017). Projected drought risk in 1.5°C and 2°C warmer climates. *Geophysical Research Letters*.

Lewis, S. L., Brando, P. M., Phillips, O. L., Van der Heijden, G. M. F., & Nepstad, D. (2011). The 2010 Amazon Drought. *Science*, *331*, 554.

McKee, T. B., Doesken, N. J., & Kleist, J. (1993). The relationship of drought frequency and duration to time scales. In *8th Conference on Applied Climatology* (pp. 179–184).

Meehl, G. A., Stocker, T. F., Collins, W. D., Friedlingstein, P., Gaye, A. T., Gregory, J. M., et al. (2007). Global Climate Projections. In S. Solomon, D. Qin, M. Manning, Z. Chen, M. Marquis, K. B. Averyt, et al. (Eds.), *Climate Change 2007: The Physical Science Basis. Contribution of Working Group I to the Fourth Assessment Report of the Intergovernmental Panel on Climate Change* (pp. 1412–1416). Cambridge, United Kingdom and New York, NY, USA: Cambridge University Press.

Milly, P. C. D., & Dunne, K. A. (2016). Potential evapotranspiration and continental drying. *Nature Climate Change*, *6*, 946–949.

Mirzabaev, A., Wu, J., Evans, J., Garcia-Oliva, F., Hussein, I. A. G., Iqbal, M. M., et al. (2019). Desertification. In *Climate change and land. An IPCC Special Report on climate change, desertification, land degradation, sustainable land management, food security, and greenhouse gas fluxes in terrestrial ecosystems* (p. 174).

O'Neill, B. C., Tebaldi, C., Van Vuuren, D. P., Eyring, V., Friedlingstein, P., Hurtt, G., et al. (2016). The Scenario Model Intercomparison Project (ScenarioMIP) for CMIP6. *Geoscientific Model Development*, *9*, 3461–3482.

Orlowsky, B., & Seneviratne, S. I. (2013). Elusive drought: Uncertainty in observed trends and short-and long-term CMIP5 projections. *Hydrology and Earth System Sciences*, *17*, 1765–1781.

Orth, R., & Seneviratne, S. I. (2012). Analysis of soil moisture memory from observations in Europe. *Journal of Geophysical Research Atmospheres*, *117*, 1–19.

Park, C.-E., Jeong, S.-J., Joshi, M., Osborn, T. J., Ho, C.-H., Piao, S., et al. (2018). Keeping global warming within 1.5 °C constrains emergence of aridification. *Nature Climate Change*, *8*, 70-74.

Pendergrass, A. G., Knutti, R., Lehner, F., Deser, C., & Sanderson, B. M. (2017). Precipitation variability increases in a warmer climate. *Scientific Reports*, *7*, 1–9.

Roderick, M. L., & Farquhar, G. D. (2002). The cause of decreased pan evaporation over the

past 50 years. *Science*, *298*, 1410–1411.
Roderick, M. L., Sun, F., Lim, W. H., & Farquhar, G. D. (2014). A general framework for understanding the response of the water cycle to global warming over land and ocean. *Hydrology and Earth System Sciences*, *18*, 1575–1589.
Saleska, S. R., Didan, K., Huete, A. R., & da Rocha, H. R. (2007). Amazon Forests Green-Up During 2005 Drought. *Science*, *318*, 2007–2007.
Scheff, J. (2018). Drought Indices, Drought Impacts, CO_2, and Warming: a Historical and Geologic Perspective. *Current Climate Change Reports*, 1–8.
Schneider, U., Ziese, M., Meyer-Christoffer, A., Finger, P., Rustemeier, E., & Becker, A. (2016). The new portfolio of global precipitation data products of the Global Precipitation Climatology Centre suitable to assess and quantify the global water cycle and resources. *Proceedings of the International Association of Hydrological Sciences*, *374*, 29–34.
Sheffield, J, & Wood, E. (2011). *Drought: past problems and future scenarios*. London, United Kingdom: Earthscan.
Sheffield, Justin, Wood, E. F., & Roderick, M. L. (2012). Little change in global drought over the past 60 years. *Nature*, *491*, 435–438.
Sherwood, S., & Fu, Q. (2014). A drier future? *Science*, *343*, 737–739.
Sillmann, J., Kharin, V. V., Zwiers, F. W., Zhang, X., & Bronaugh, D. (2013). Climate extremes indices in the CMIP5 multimodel ensemble: Part 2. Future climate projections. *Journal of Geophysical Research Atmospheres*, *118*, 2473–2493.
Sun, F., Roderick, M. L., & Farquhar, G. D. (2012). Changes in the variability of global land precipitation. *Geophysical Research Letters*, *39*, 1–6.
Swann, A. L. S., Hoffman, F. M., Koven, C. D., & Randerson, J. T. (2016). Plant responses to increasing CO_2 reduce estimates of climate impacts on drought severity. *Proceedings of the National Academy of Sciences*, *113*, 10019–10024.
Taylor, K. E., Stouffer, R. J., & Meehl, G. a. (2012). An Overview of CMIP5 and the Experiment Design. *Bulletin of the American Meteorological Society*, *93*, 485–498.
Trenberth, K. E., Dai, A., Schrier, G. Van Der, Jones, P. D., Barichivich, J., Briffa, K. R., & Sheffield, J. (2014). Global warming and changes in drought. *Nature Climate Change*, *4*, 17–22.
Ukkola, A. M., & Prentice, I. C. (2013). A worldwide analysis of trends in water-balance evapotranspiration. *Hydrology and Earth System Sciences*, *17*, 4177–4187.
Ukkola, A. M., Pitman, A. J., De Kauwe, M. G., Abramowitz, G., Herger, N., Evans, J. P., & Decker, M. (2018). Evaluating CMIP5 model agreement for multiple drought metrics. *Journal of Hydrometeorology*, *19*, 969–988.
Vicente-Serrano, S. M., Beguería, S., López-Moreno, J. I., Vicente-Serrano, S. M., Beguería, S., & López-Moreno, J. I. (2010). A Multiscalar Drought Index Sensitive to Global Warming: The Standardized Precipitation Evapotranspiration Index. *Journal of Climate*, *23*, 1696–1718.
van Vuuren, D. P., Edmonds, J., Kainuma, M., Riahi, K., Thomson, A., Hibbard, K., et al. (2011). The representative concentration pathways: an overview. *Climatic Change*, *109*, 5–31.
Yang, Y., Roderick, M. L., Zhang, S., McVicar, T. R., & Donohue, R. J. (2019). Hydrologic implications of vegetation response to elevated CO_2 in climate projections. *Nature Climate Change*, *9*, 44–48.

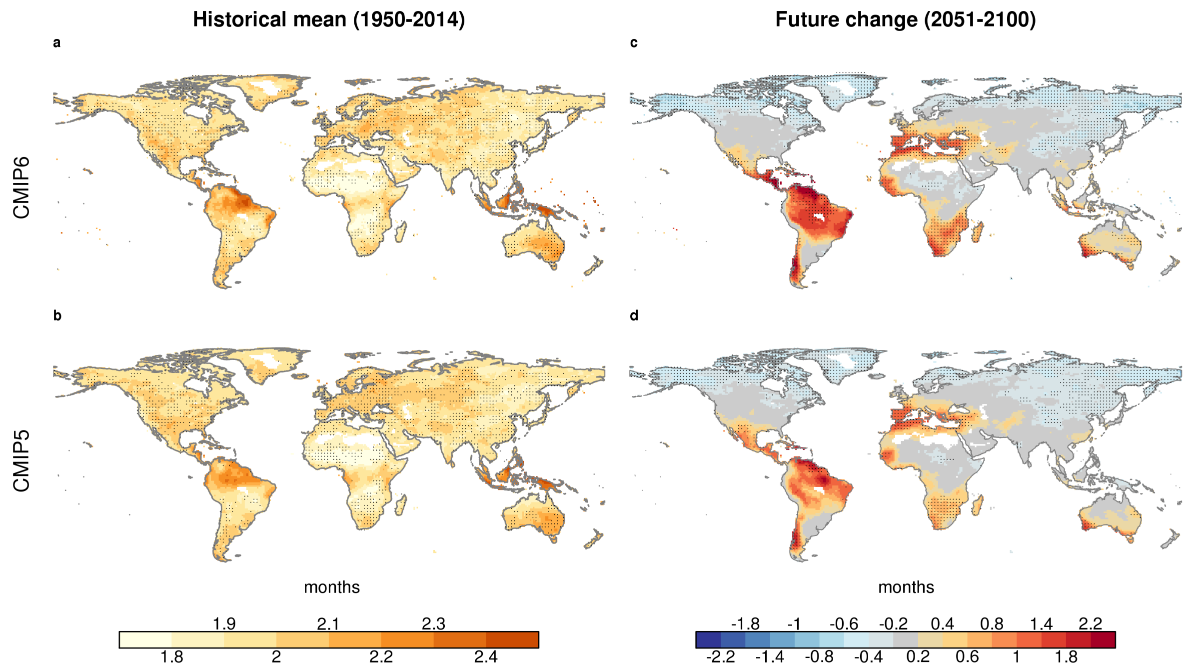

Figure 1. Projected changes in drought duration. Multi-model mean historical drought duration for nine (a) CMIP6 and (b) CMIP5 models during the 1950-2014 baseline period. Stippling indicates where ≥75% of models are within 10% of the observed mean (34% of land area in a and 32% in b) (see Figure S3a for observed mean duration). (c) Projected future change in drought duration from 1950-2014 to 2051-2100 for CMIP6 and (d) CMIP5 using the 8.5 W m^{-2} scenario. Stippling indicates where the magnitude of the multi-model mean future change exceeds the inter-model standard deviation (45% of land area in c and 31% in d).

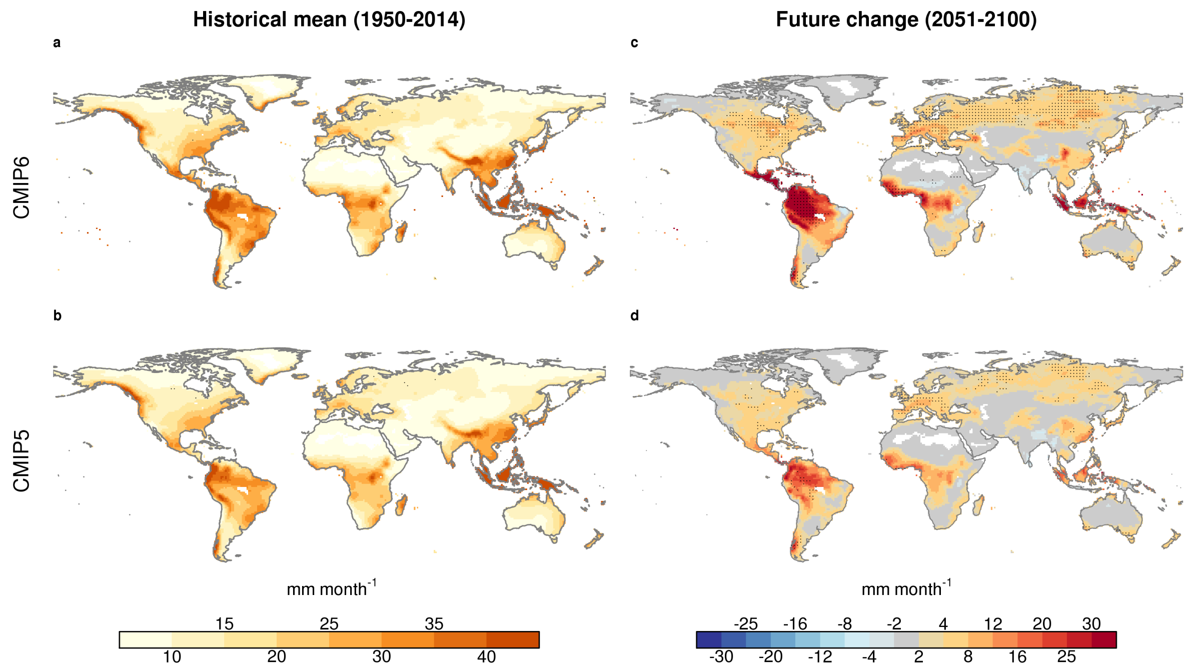

Figure 2. Projected changes in drought intensity. Multi-model mean historical drought intensity for nine (a) CMIP6 and (b) CMIP5 models during the 1950-2014 baseline period. Stippling indicates where ≥75% of models are within 10% of the observed mean (0.2% of land area in a and 0.16% in b) (see Figure S3b for observed mean intensity). (c) Projected future change in drought intensity from 1950-2014 to 2051-2100 for CMIP6 and (d) CMIP5 using the 8.5 W m^{-2} scenario. Stippling indicates where the magnitude of the multi-model mean future change exceeds the inter-model standard deviation (26% of land area in c and 10% in d).

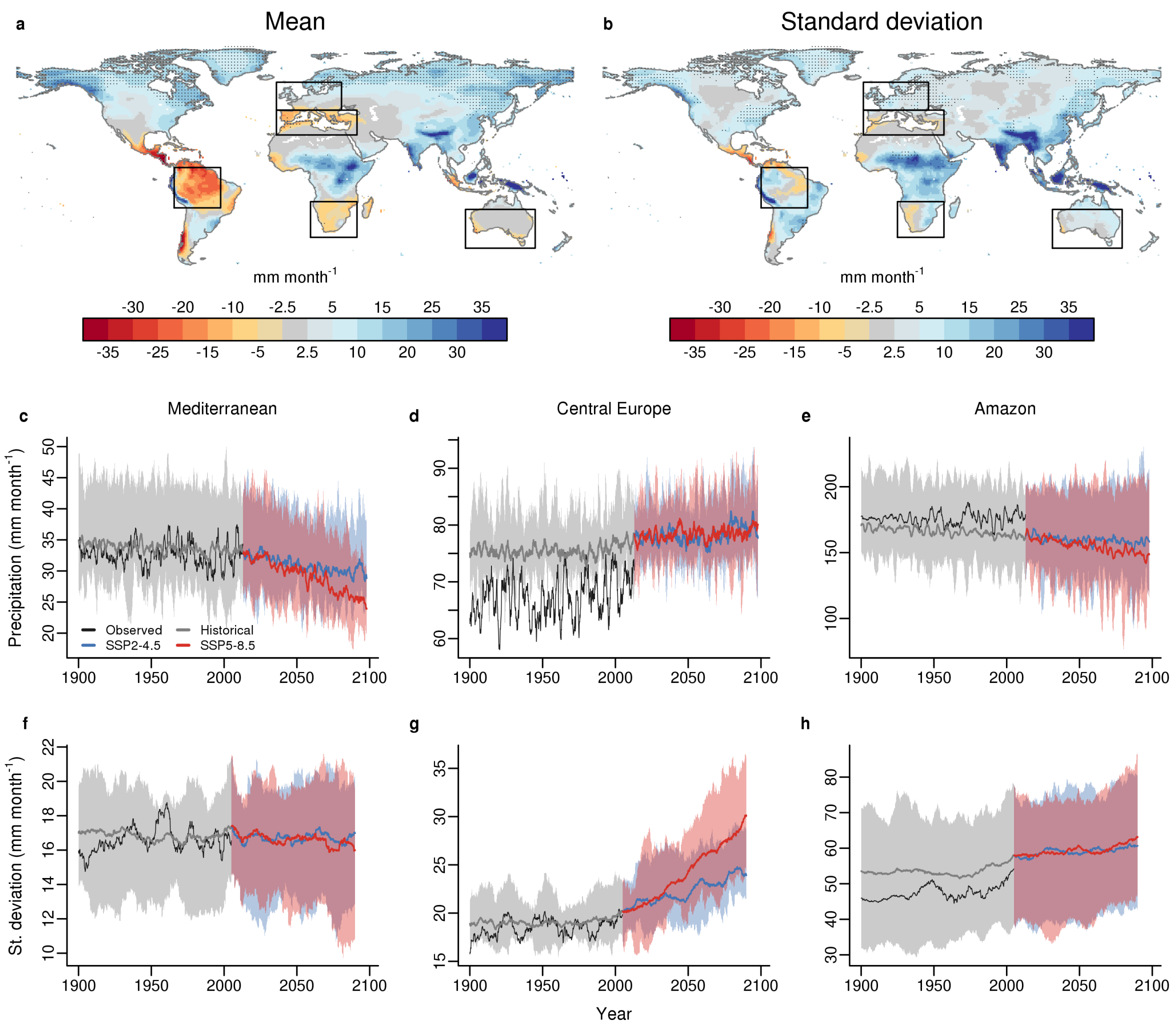

Figure 3. Projected changes in monthly precipitation mean and variability. (a) Projected multi-model mean change in monthly mean precipitation and (b) standard deviation for nine CMIP6 models under the 8.5 W m^{-2} scenario compared to the 1950-2014 period. Stippling indicates where the magnitude of the multi-model mean future change exceeded the inter-model standard deviation (24% of land area in a and 21% in b). Data for the historical and future periods were linearly detrended prior to calculating the standard deviation to remove effects from changes in the mean. (c-e) show a time series of monthly mean precipitation for the Mediterranean, central Europe and Amazon regions, respectively, smoothed using a 24-month running window. (f-h) show a time series of 10-year running standard deviation of monthly precipitation for the same regions. In (c-f) the shading shows the full model range and the solid lines the multi-model means. For observations, the mean of the three observed products is shown. Data for the southern African and Australian regions are shown in Supplementary Figure S6.

Geophysical Research Letters

Supporting Information for

Robust future changes in meteorological drought in CMIP6 projections despite uncertainty in precipitation

Anna M. Ukkola[1], Martin G. De Kauwe[2], Michael L. Roderick[1], Gab Abramowitz[2] and Andrew J. Pitman[2]

[1]ARC Centre of Excellence for Climate Extremes and Research School of Earth Sciences, Australian National University, Canberra, ACT, Australia

[2]ARC Centre of Excellence for Climate Extremes and Climate Change Research Centre, University of New South Wales, Sydney, NSW, Australia

Contents of this file

Figures S1-S12
Tables S1-S2

Table S1. CMIP5 and CMIP6 models used in this study. Where possible, the equivalent models from CMIP5 and CMIP6 were chosen and otherwise available models by the same institution were matched. Resolution shows the model resolution as degrees latitude and longitude, respectively. For CMIP6 models, *gn* indicates native resolution and *gr* regridded resolution. Ensembles shows the individual model ensemble members used in this study for all historical and future simulations.

CMIP6			**CMIP5**		
Model	**Resolution**	**Ensembles**	**Model**	**Resolution**	**Ensembles**
BCC-CSM2-MR	1.12, 1.13 (gn)	r1i1p1f1	BCC-CSM1-1	2.79, 2.81	r1i1p1
CanESM5	2.79, 2.81 (gn)	r1i1p1f1	CanESM2	2.79, 2.81	r1i1p1, r2i1p1, r3i1p1, r4i1p1, r5i1p1
CESM2-WACCM	0.94, 1.25 (gn)	r1i1p1f1	CESM1-WACCM	1.88, 2.5	r2i1p1, r3i1p1, r4i1p1
CNRM-CM6-1	1.40, 1.41 (gr)	r1i1p1f2, r2i1p1f2, r3i1p1f2, r4i1p1f2, r5i1p1f2, r6i1p1f2	CNRM-CM5	1.40, 1.41	r1i1p1
GFDL-CM4	1.00, 1.25 (gr)	r1i1p1f1	GFDL-CM3	2.00, 2.50	r1i1p1
IPSL-CM6A-LR	1.27, 2.50 (gr)	r1i1p1f1	IPSL-CM5A-LR	1.89, 3.75	r1i1p1, r2i1p1, r3i1p1, r4i1p1
MIROC6	1.40, 1.41 (gn)	r1i1p1f1	MIROC5	1.40, 1.41	r1i1p1, r2i1p1, r3i1p1
MRI-ESM2-0	1.12, 1.13 (gn)	r1i1p1f1	MRI-CGCM3	1.12, 1.13	r1i1p1
UKESM1-0-LL	1.25, 1.86 (gn)	r1i1p1f2, r2i1p1f2, r3i1p1f2, r4i1p1f2, r8i1p1f2	HadGEM2-ES	1.25, 1.88	r1i1p1, r2i1p1, r3i1p1, r4i1p1

Table 2: Additional CMIP5 models used in Supplementary Figure S1. Resolution shows the model resolution as degrees latitude and longitude, respectively. Ensembles shows the individual model ensemble members used in this study for all historical and future simulations.

Model	Resolution	Ensembles
ACCESS1-0	1.25, 1.88	r1i1p1
ACCESS1-3	1.25, 1.88	r1i1p1
BNU-ESM	2.79, 2.81	r1i1p1
CCSM4	0.94, 1.25	r1i1p1, r2i1p1, r3i1p1, r4i1p1, r5i1p1, r6i1p1
CESM1-BGC	0.94, 1.25	r1i1p1
CESM1-CAM5	0.94, 1.25	r1i1p1, r2i1p1, r3i1p1
CSIRO-Mk3-6-0	1.87, 1.88	r1i1p1, r2i1p1, r3i1p1, r4i1p1, r5i1p1, r6i1p1, r7i1p1, r8i1p1, r9i1p1, r10i1p1
FGOALS-g2	2.79, 2.81	r1i1p1
GFDL-ESM2G	2.02, 2.00	r1i1p1
GFDL-ESM2M	2.02, 2.50	r1i1p1
GISS-E2-H	2.00, 2.50	r1i1p1, r1i1p2, r1i1p3, r2i1p1, r2i1p3
GISS-E2-R	2.00, 2.50	r1i1p1, r1i1p2, r1i1p3, r2i1p1, r2i1p3
HadGEM2-CC	1.25, 1.88	r1i1p1
INMCM4	1.50, 2.00	r1i1p1
IPSL-CM5A-MR	1.27, 2.50	r1i1p1
IPSL-CM5B-LR	1.89, 3.75	r1i1p1
MIROC-ESM	2.79, 2.81	r1i1p1
MIROC-ESM-CHEM	2.79, 2.81	r1i1p1
MPI-ESM-LR	1.87, 1.88	r1i1p1, r2i1p1, r3i1p1
MPI-ESM-MR	1.87, 1.88	r1i1p1
NorESM1-M	1.89, 2.50	r1i1p1
NorESM1-ME	1.89, 2.50	r1i1p1

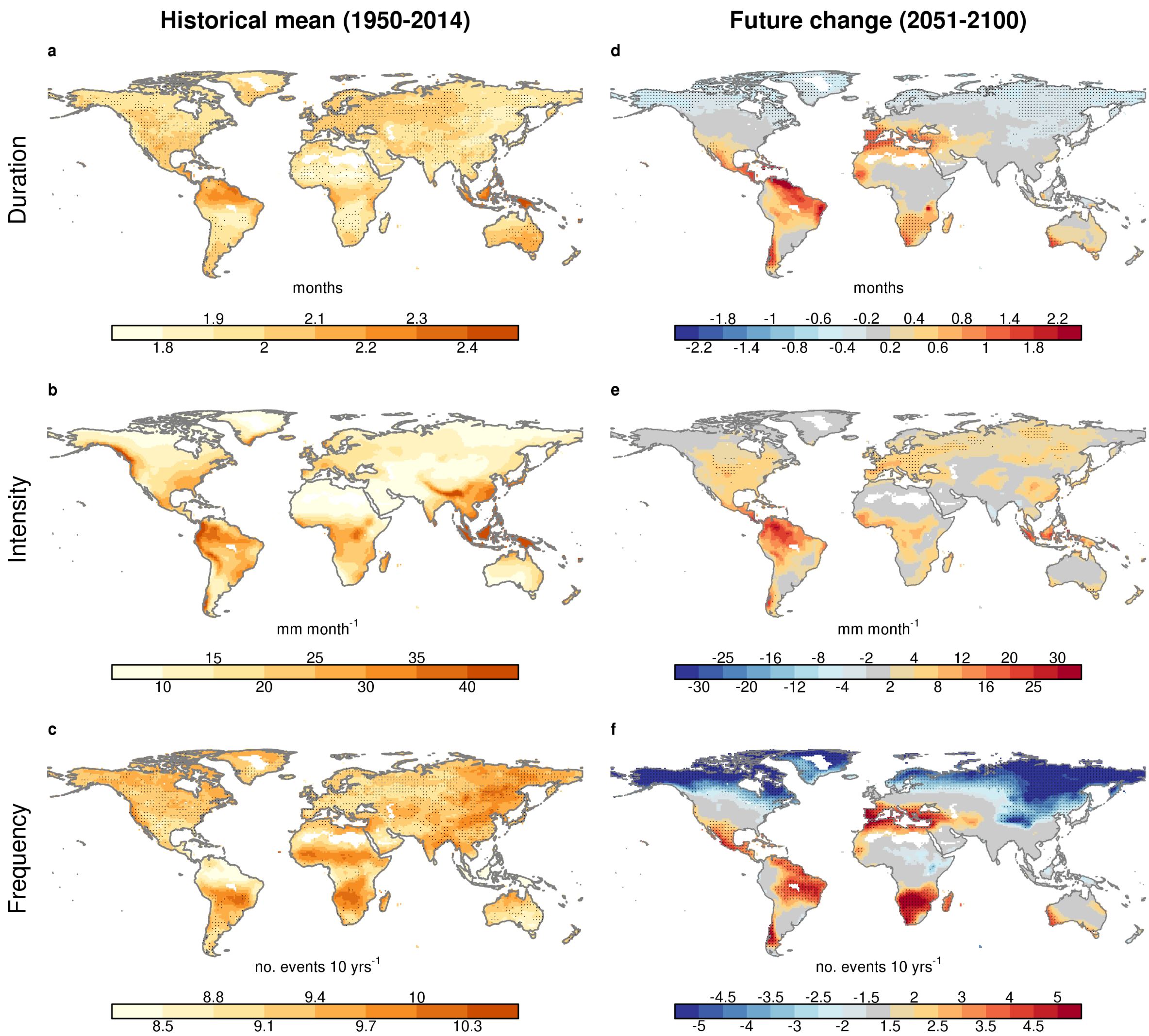

Fig. S1. Projected changes in drought metrics in the full CMIP5 archive. (a,b,c) the multi-model mean historical drought duration, intensity and frequency, respectively, for 31 CMIP5 models during the 1950-2014 baseline period. Stippling indicates where ≥75% of models are within 10% of the observed mean (27% of land area in a, 0% in b and 26% in c) (see Figure S3 for observed metrics). (d,e,f) projected future change in drought duration, intensity and frequency, respectively, relative to the historical mean using the 8.5 W m^{-2} scenario. Stippling indicates where the magnitude of the multi-model mean future change exceeds the inter-model standard deviation (26% of land area in d, 8% in e and 46% in f).

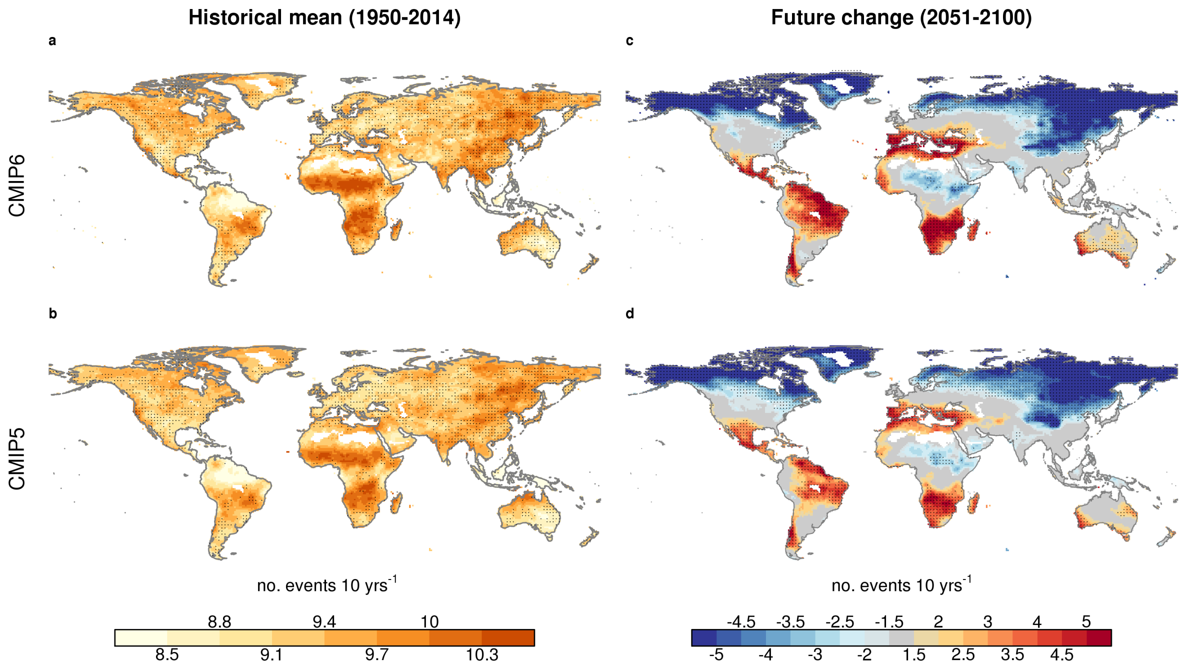

Fig. S2. Projected changes in drought frequency. (a) multi-model mean historical drought frequency for nine CMIP6 and (b) CMIP5 models during the 1950-2014 baseline period. Stippling indicates where ≥75% of models are within 10% of the observed mean (33% of land area in a and 29% in b) (see Figure S3c for observed mean frequency). (c) projected future change in drought frequency relative to the historical mean for CMIP6 and (d) CMIP5 using the 8.5 W m^{-2} scenario. Stippling indicates where the magnitude of the multi-model mean future change exceeds the inter-model standard deviation (57% of land area in c and 51% in d).

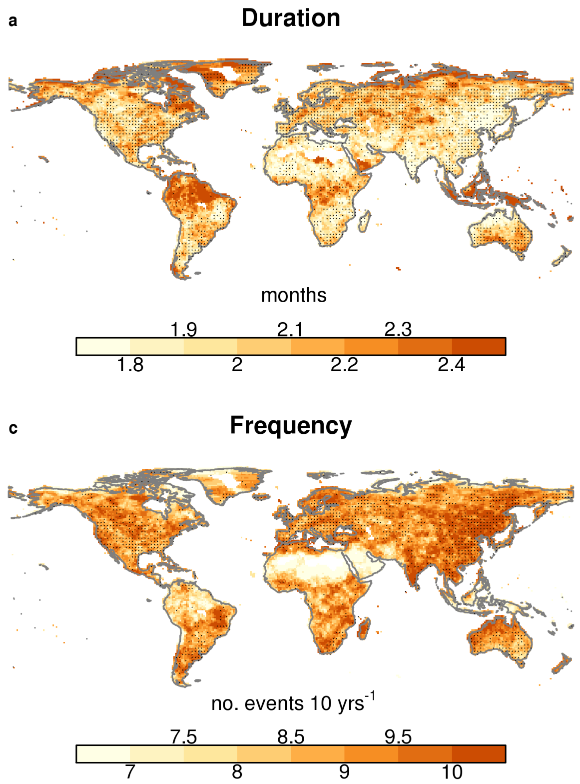

Fig. S3. Mean observed drought metrics during the 1950-2014 baseline period. Mean historical drought (a) duration (b) intensity and (c) frequency for the three observed precipitation products. Stippling indicates where all three observed datasets are within 10% of the mean.

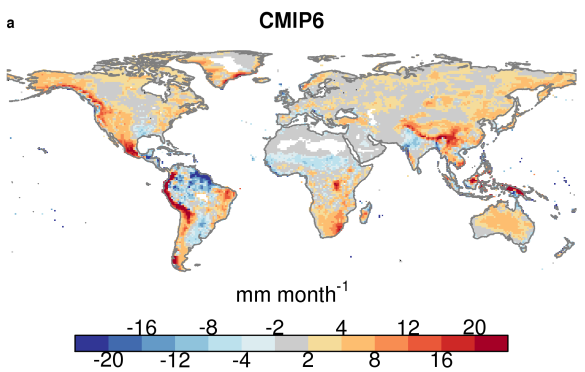

Fig. S4. Bias in historical mean drought intensity. Difference in (a) CMIP6 and (b) CMIP5 ensemble mean drought intensity compared to the mean of the three observational products during the 1950-2014 baseline period.

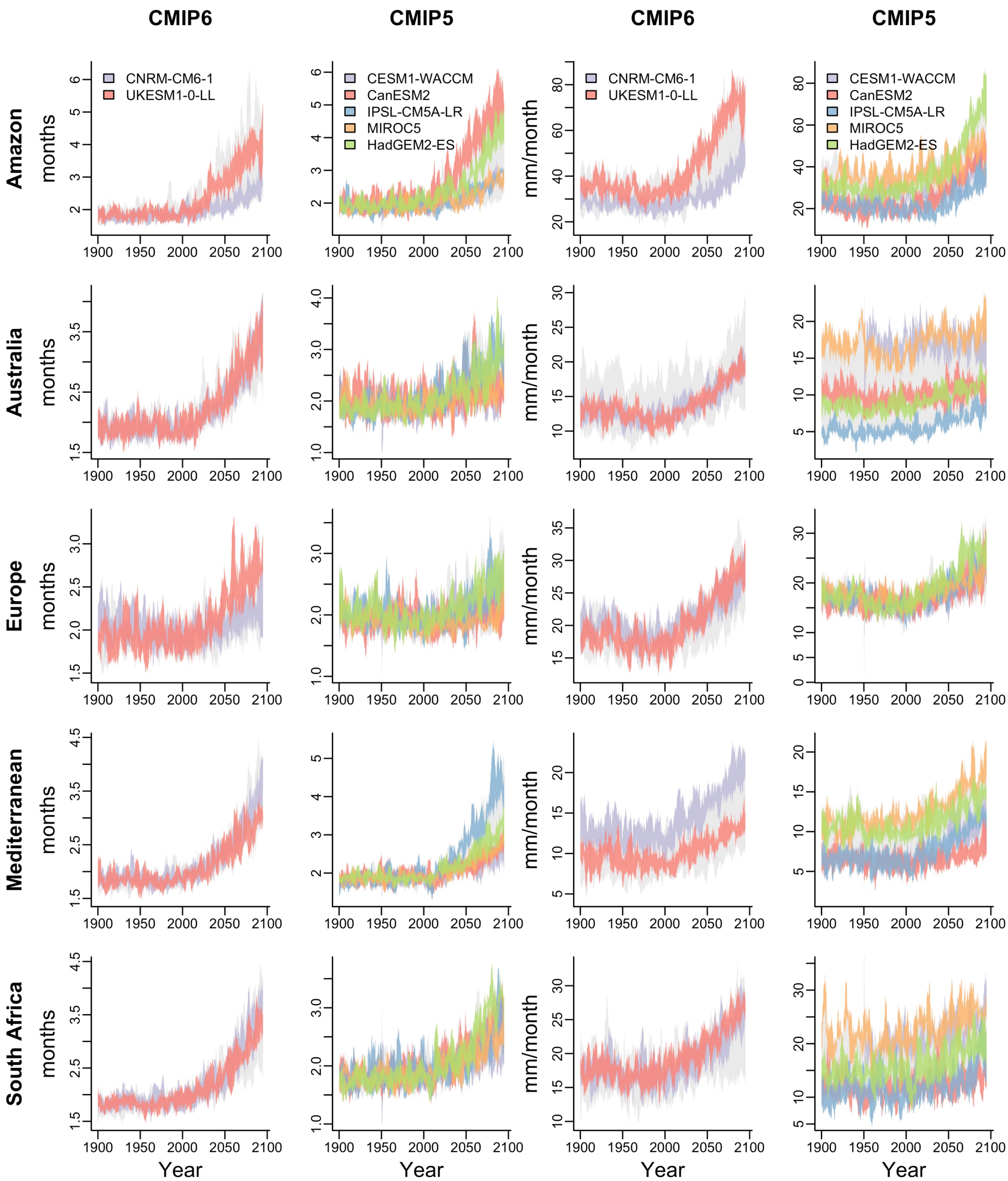

Fig. S5. Range in drought projections due to internal variability in five key regions. The two left-hand panels show time series in drought duration for CMIP6 and CMIP5, respectively, and the two right-hand panels that for drought intensity for the SSP5-8.5 and RCP8.5 emissions scenarios. The coloured shading shows the range across individual ensemble members for each model and the grey shading shows the full range across all models and ensembles. See Table S1 for ensemble members and Figure 3 for regions.

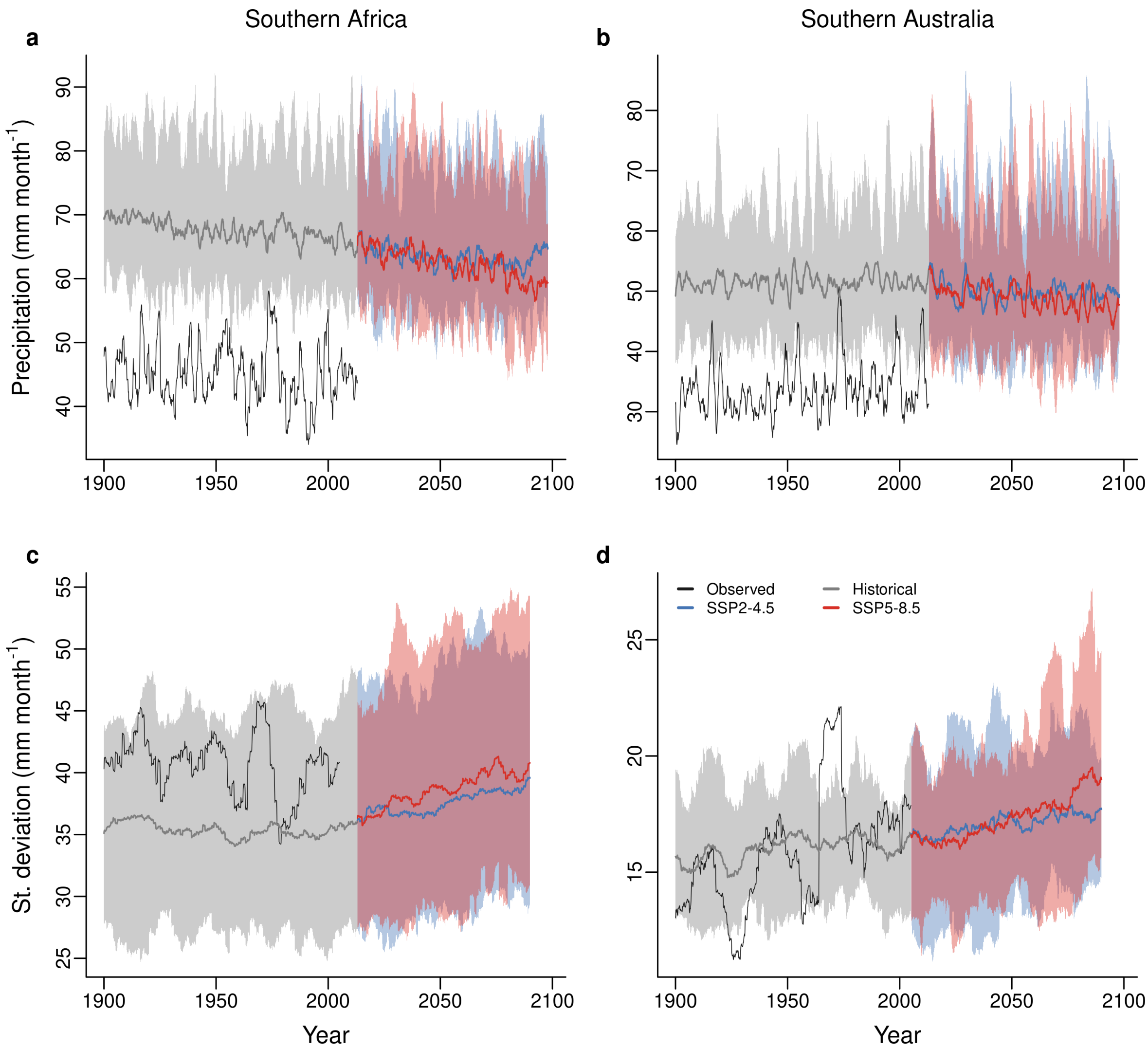

Fig. S6. Projected changes in monthly precipitation mean and variability in southern African and Australian regions. (a-b) show a time series of monthly mean precipitation for the southern African and southern Australian regions, respectively, smoothed using a 24-month running window. (c-d) show a time series of 10-year running standard deviation for the same regions. In (a-d) the shading shows the full model range and the solid lines the multi-model means. For observations, the mean of the three observed products is shown.

Future projections of drought for the 4.5 W m^{-2} emissions scenario

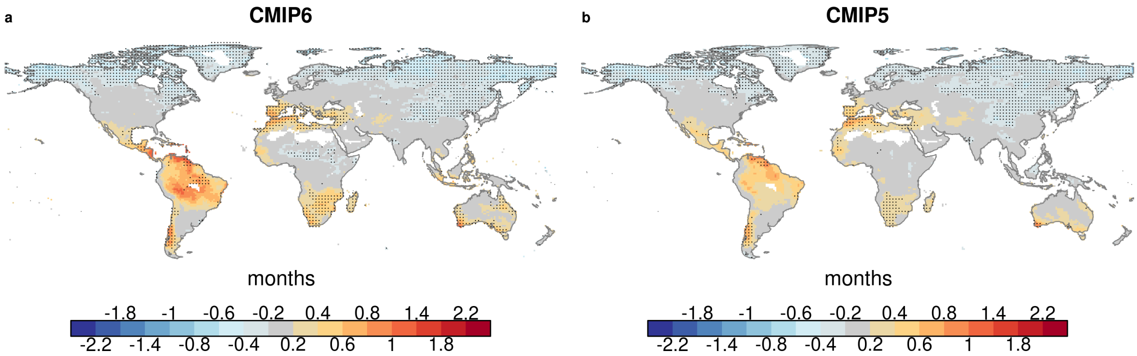

Fig. S7. Projected changes in drought duration for the 4.5 W m^{-2} emissions scenario. Projected future change in drought duration relative to the historical mean for a) CMIP6 SSP2-4.5 scenario and b) CMIP5 RCP4.5 scenario. Stippling indicates where the magnitude of the multi-model mean future change exceeds the inter-model standard deviation (36% of land area in a and 29% in b).

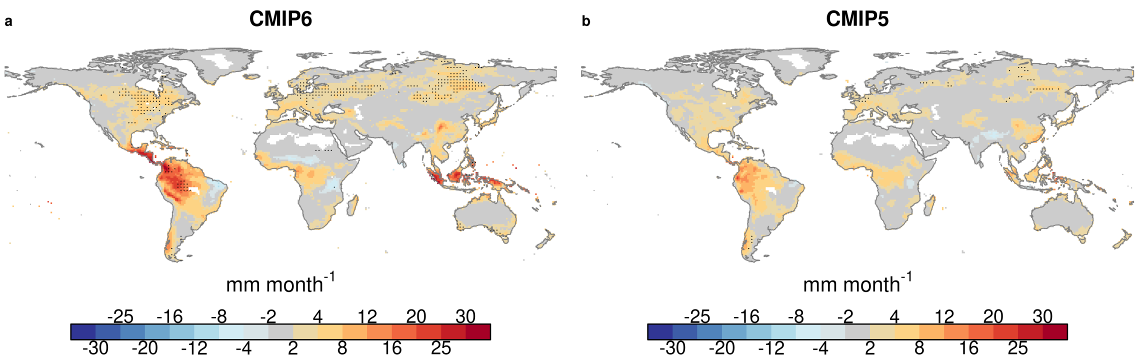

Fig. S8. Projected changes in drought intensity for the 4.5 W m^{-2} emissions scenario. Projected future change in drought intensity relative to the historical mean for a) CMIP6 SSP2-4.5 scenario and b) CMIP5 RCP4.5 scenario. Stippling indicates where the magnitude of the multi-model mean future change exceeds the inter-model standard deviation (10% of land area in a and 2% in b).

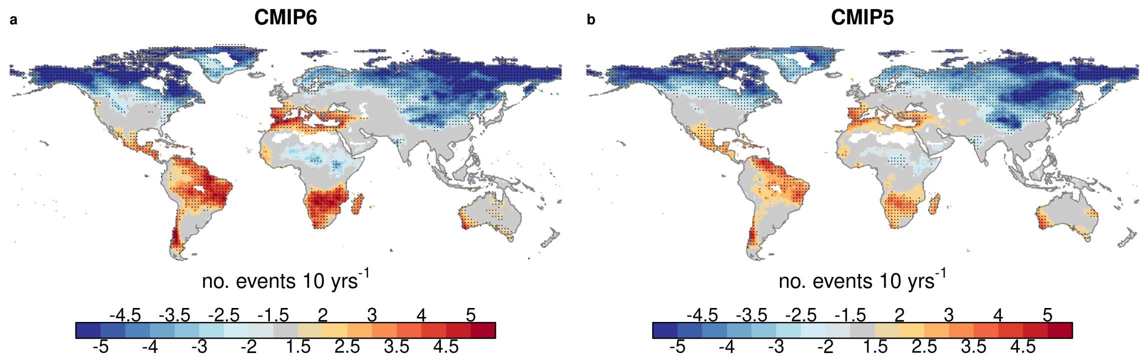

Fig. S9. Projected changes in drought frequency for the 4.5 W m^{-2} emissions scenario. Projected future change in drought frequency relative to the historical mean for a) CMIP6 SSP2-4.5 scenario and b) CMIP5 RCP4.5 scenario. Stippling indicates where the magnitude of the multi-model mean future change exceeds the inter-model standard deviation (52% of land area in a and 45% in b).

Future projections of drought using 12-month running means

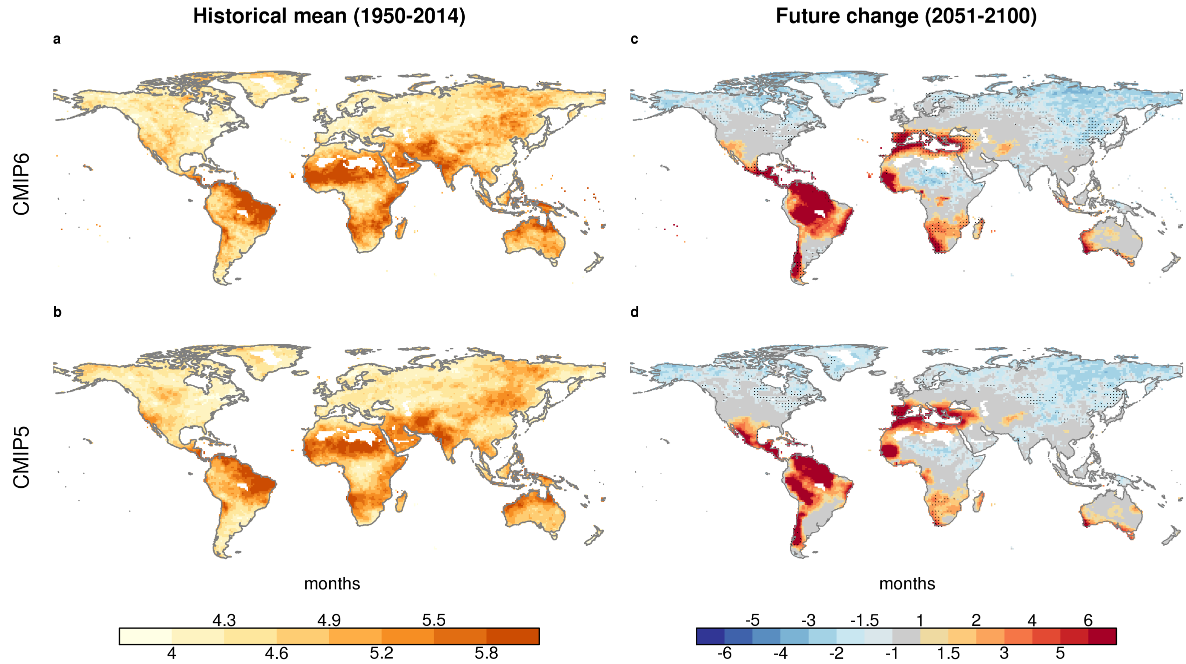

Fig. S10. Projected changes in drought duration using 12-month running means. (a) mean historical drought duration for nine CMIP6 and (b) CMIP5 models during the 1950-2014 baseline period. Stippling indicates where ≥75% of models are within 10% of the observed mean. (c) projected future change in drought duration relative to the historical mean for CMIP6 and (d) CMIP5 using the 8.5 W m^{-2} emissions scenario. Stippling indicates where the magnitude of the multi-model mean future change exceeds the inter-model standard deviation.

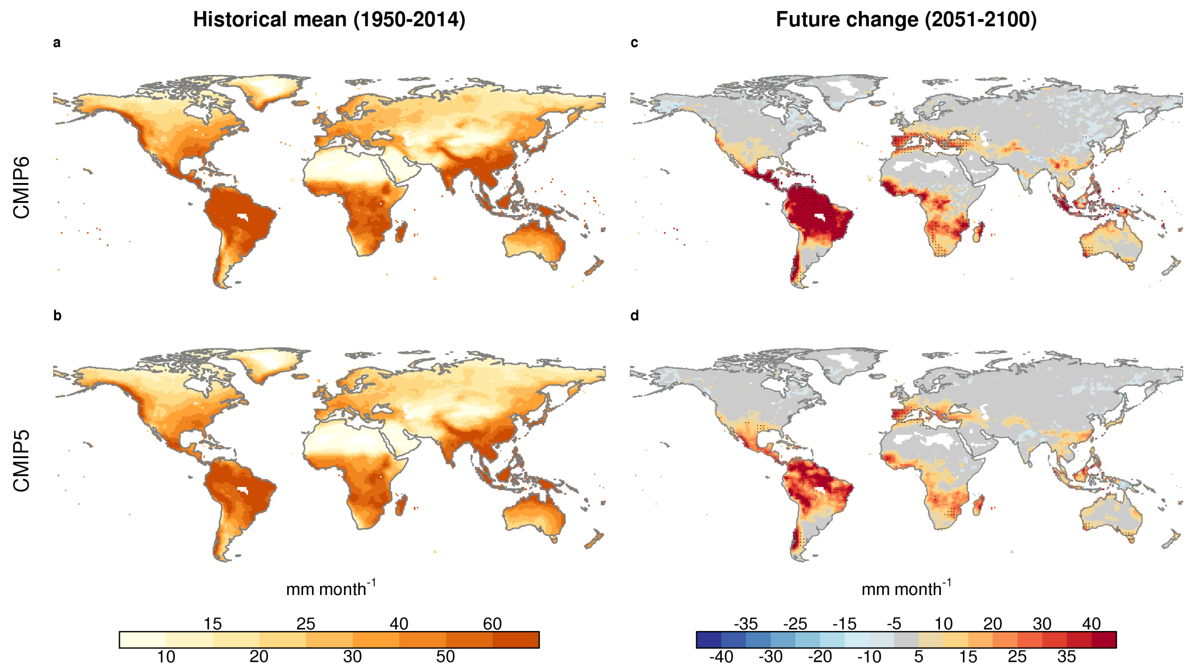

Fig. S11. Projected changes in drought intensity using 12-month running means. (a) mean historical drought intensity for nine CMIP6 and (b) CMIP5 models during the 1950-2014 baseline period. Stippling indicates where ≥75% of models are within 10% of the observed mean. (c) projected future change in drought intensity relative to the historical mean for CMIP6 and (d) CMIP5 using the 8.5 W m^{-2} emissions scenario. Stippling indicates where the magnitude of the multi-model mean future change exceeds the inter-model standard deviation.

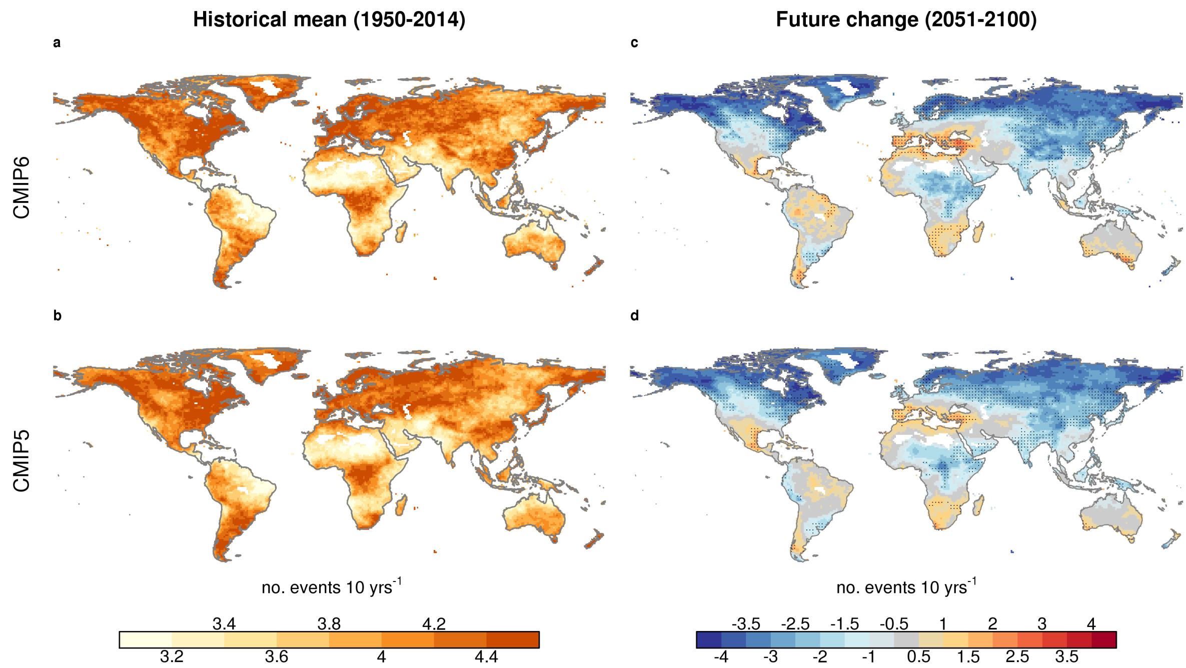

Fig. S12. Projected changes in drought frequency using 12-month running means. (a) mean historical drought frequency for nine CMIP6 and (b) CMIP5 models during the 1950-2014 baseline period. Stippling indicates where ≥75% of models are within 10% of the observed mean. (c) projected future change in drought frequency relative to the historical mean for CMIP6 and (d) CMIP5 using the 8.5 W m^{-2} emissions scenario. Stippling indicates where the magnitude of the multi-model mean future change exceeds the inter-model standard deviation.